Appl. Phys. B 68, 459–463 (1999)

Applied Physics B
Lasers
and Optics

Ultrafast carrier dynamics in laser-excited materials: subpicosecond optical studies

F. Quéré[1,*], S. Guizard[1,*], P. Martin[1], G. Petite[1], O. Gobert[2], P. Meynadier[2], M. Perdrix[2]

[1] Service de Recherches sur les Surfaces et l'Irradiation de la Matière, CEA, Centre de Saclay, 91191 Gif sur Yvette, France
[2] Service des Photons, Atomes, Molécules, CEA, Centre de Saclay, 91191 Gif sur Yvette, France

Received: 20 September 1998

Abstract. In this paper, we present measurements of the excited carrier density in various wide-band-gap oxides (SiO_2, MgO and Al_2O_3) irradiated by short laser pulses (70 fs to 1.3 ps) at intensities below and above breakdown threshold. This is achieved with the help of time-resolved interferometry in the frequency domain, which was successfully used to study the dynamics of photoexcited carriers in insulators. The results obtained under different experimental conditions, distance from the surface, pump intensities and duration, during or after the pump pulse, are discussed and compared to the models recently developed to explain optical breakdown.

PACS: 79.20.Ds; 78.47.+p

Although widely explored over the last thirty years [1–3], the problem of optical breakdown still remains an active field. This is mainly due to the spreading of laser sources delivering subpicosecond pulses with high intensities. This not only increases the technological need to produce optical materials capable of sustaining high peak power, but also opens new experimental possibilities and new fundamental questions.

Until now, most of the work has been devoted to the measurement of the breakdown threshold as a function of wavelength or pulse duration (τ) [3–6]. These studies have shown that the breakdown threshold deviates from a thermally driven $\tau^{1/2}$ law for pulse durations shorter than 50 or 20 ps, indicating different behaviour for short and ultrashort laser pulses.

Such breakdown threshold measurements are, of course, particularly important for applications. They strongly depend, however, on the criteria chosen to determine a threshold: single or multiple shots, microscopic or macroscopic damage, and they can be influenced by extrinsic parameters like sample quality or surface preparation. Moreover, the fundamental mechanisms involved in optical damage are numerous, making the modelling of this process a difficult task. It is therefore highly desirable to get precise quantitative information on basic phenomena.

* Corresponding author. (E-mail: quere@DRECAM.cea.fr)

For instance Jones et al. [2] have investigated phonon emission at laser intensities below breakdown and have shown the importance of electron–phonon collisions, which can heat the lattice close to the melting temperature. These measurements also emphasise the role of multiphoton excitation, showing that this process dominates over avalanche ionization at least up to intensities close to breakdown. They also experimentally demonstrated the process of electron heating by laser [7], which was later directly observed by measuring the kinetic energy of photoelectrons [8].

In this context, pump–probe techniques with high temporal resolution are promising in investigations of the fundamental mechanisms occurring during or just after the pump pulse. To our knowledge, only one published result used such techniques to measure the change of reflectivity at the surface of laser-irradiated dielectric materials [9].

In this paper we present the measurements of excitation densities in various wide-band-gap oxides (SiO_2, MgO and Al_2O_3) excited by laser pulses of variable duration (80 fs to 1.3 ps) at intensities below and above breakdown threshold. The time-resolved interference method is presented in the next section, the main results are given and commented on in the following section.

1 Experimental principle and set-up

The experimental set-up has already been described in detail [10]; we will briefly recall the principle of the measurements. A high-intensity pump pulse creates initially free electron–hole pairs. The probe system consists of two identical pulses separated by a fixed time delay and colinearly propagating, one (the reference pulse) crossing the sample before and the second (probe pulse) after the pump pulse. The reference and probe pulses are sent into a spectrometer, with the pump–probe interaction region in the sample imaged at the entrance slit. The spectrometer acts as a temporal stretcher. At the exit, the pulse duration is larger than the time delay that separates them and interferences are readily observed. The fringe separation ($\Delta\omega$) is inversely proportional to the time delay (Δt) that separates the two

probe pulses. The resolution of the spectrometer thus gives an upper limit for Δt. In our case, this time delay is set to 10 ps. The modification of the refractive index Δn induces for the probe pulse a phase shift $\Delta\Phi$ which is proportional to the length L over which the pump and probe beams are overlapped. Since Δn depends on the pump laser intensity, which has a Gaussian profile, the measured phase shift exhibits a corresponding dependence $\Delta\Phi(r)$ along the axis of the entrance slit. It can thus be writen: $\Delta\Phi(r) = 2\pi\Delta n(r)L/\lambda$, where λ is the probe wavelength. This phase shift induces a distortion of the fringe pattern, while absorption of the probe pulse reduces the fringes contrast. Both quantities (phase shift and absorption) are obtained by a Fourier analysis of the interference pattern at the output of the spectrometer.

The laser is a Ti-Sa system with three amplification stages: one regenerative and two multipass amplifiers, delivering 70 fs pulses with energies up to 100 mJ. The output beam is split in two parts, which are each sent into different compressors. This allows us to use different pulse durations for the probe and pump. We use the second harmonic (395 nm) as a probe, and for the pump we use a part of the fundamental (790 nm, 1.57 eV photons).

The pump beam is spatially filtered, to get a soft Gaussian profile and limit the spatial fluctuation of the pump beam at the focus. The quality of the pump beam profile and its size can be measured in situ during the experiment with the help of the Kerr effect, which is observed when the probe and pump cross the sample at the same time (Fig. 1a). As explained in the next section, the measured phase shift in this case is proportional to the pump intensity. Similarly, we measure for each experiment the pulse duration (Fig. 1b). Finally, in energy-dependent measurements, the pump energy is measured at each laser shot with a calibrated photodiode. All parameters necessary to determine the intensity are thus precisely known. For other measurements, laser shots whose energy falls outside a given window (usually $\pm 5\%$) are rejected to limit the pulse to pulse fluctuations.

If the overlap between the pump and probe beams is too long, it leads to complete absorption of the probe pulse. We therefore focus the pump beam tightly (FWHM (full width at half maximum) in the range 8 to 15 μm) and the beams are incident at 45° on both sides of the normal to the sample. An important aspect of the measurements presented below is the precise knowledge of the region where the two beams overlap in the sample. Since we image the interaction region at the entrance slit of the spectrometer, we can precisely control this parameter. In particular, we can align the beams and the imaging system such that they cross just at the surface. Taking into account the geometry of the experiment, this leads to an overlap of about half the diameter of the pump beam, starting from the surface. We can also shift the image of the probe beam on the entrance slit laterally such that the part of the probe that we analyse has crossed the pump beam inside the sample at a given depth. We will present below the results of such measurements for different depths.

The surface of the samples have been superpolished to limit the influence of surface roughness – to which we believe our measurements are not very sensitive anyway. The samples are 500 μm to 1 mm thick. They are mounted on a automated three-axis translation stage and moved after each laser shot to work on a fresh area.

After crossing the sample, the probe beam is split into two parts, one going to the spectrometer, the other to a video camera. We use this image of the sample's surface to monitor any permanent damage after each laser shot. The result of this check (breakdown or no breakdown) is saved together with the data file. Although breakdown threshold measurement is not our aim, this gives an indication of the damage with size smaller or comparable to the diameter of the pump beam. The values we find for this "breakdown threshold" are higher than published data [3–6] by a factor ranging from two to ten. This discrepency can be explained by the fact that we are making single shot measurements, and that, given the magnification ($\times 73$), the size of damage that we can observe is of the order of 1 or 2 μm.

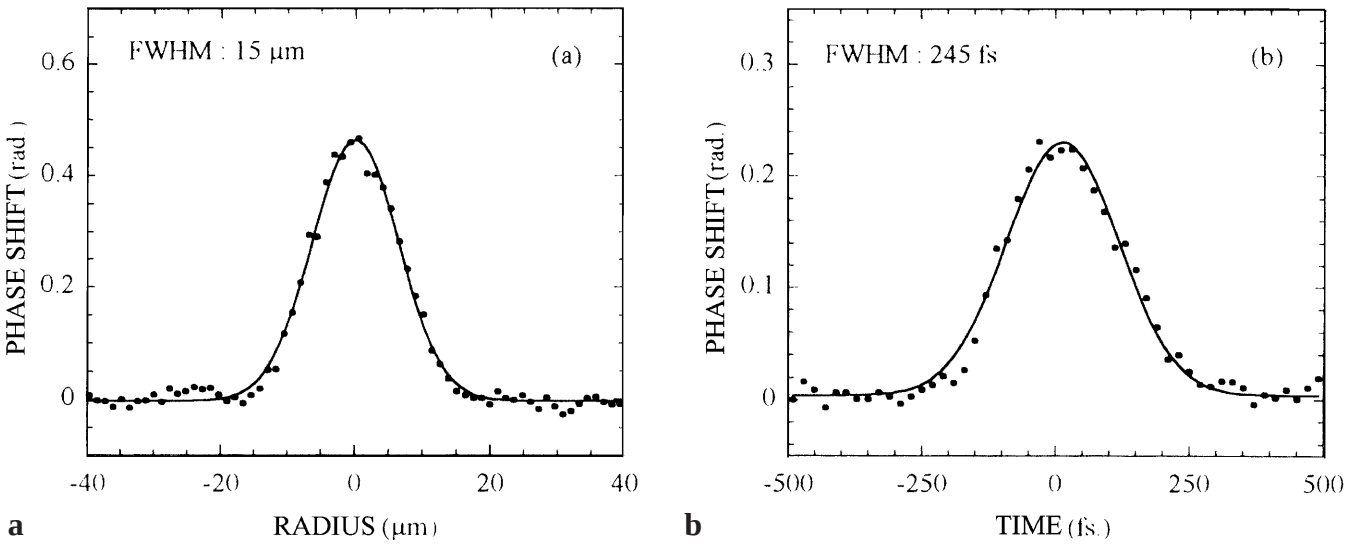

Fig. 1a,b. Spatial (**a**) and temporal (**b**) profile of the pump beam, measured via the Kerr effect in Al_2O_3 and SiO_2, respectively. Curve **b** gives the correlation function of pump and probe, from which we can deduce the probe-pulse duration (230 fs), the pump-pulse duration (80 fs in this case) being measured independently with an autocorrelator

2 Results and discussion

Let us first recall the physical origin of the refractive-index change, and thus of the phase shift that we measure in our experiment. A simple model describing the real part of the refractive index gives [10]

$$\Delta n = n_2 I(t) + \frac{e^2}{2n_0\varepsilon_0}\left(-\frac{N_f(t)}{m^*\left(\omega^2+\omega_c^2\right)}+\sum_i \frac{N_{t_i}(t)\, f_{t_i}}{m\left(\omega_{t_i}^2-\omega^2\right)}\right) \quad (1)$$

The first term is due to the nonlinear polarization induced in the sample by the pump pulse (optical Kerr effect) and is proportional to its intensity. This effect will last only as long as the pump and probe pulses are together in the sample and it gives a positive phase shift since the nonlinear refractive index n_2 is positive at our probe wavelength. The second term is due to "free" carriers and is derived from a Drude model. It is proportional to the excitation density N_f, and always negative. ω is the probe laser frequency, and ω_c the electron–phonon collision rate. Finally, the last term represents the contribution of trapped carriers and must be taken into account in materials like alkali halides or SiO_2, where electron–hole pairs rapidly trap to form self-trapped excitons. In this term ω_{t_i} and f_{t_i} are the effective frequencies and oscillator strength simulating the absorption bands for the localized electronic states. The sign of each of these terms depends on the position of the probe frequency with respect to the maximum of the absorption spectrum: it will be positive on the red side ($\omega < \omega_{t_i}$), and negative on the blue side ($\omega > \omega_{t_i}$).

We have performed two types of measurements: as a function of time for a given laser intensity and as a function of intensity for a given time delay, just at the end of the pump pulse. At laser intensities above damage threshold, there is no doubt that a high-density plasma is generated at the surface of the sample. One may wonder if atoms, ions or electrons may migrate over significant distances during the longest pulses that we used in the experiments (1.3 ps), thus modifying the effective length over which we measure the phase shift. To check this point, we have performed measurements as a function of time at intensities below and above threshold. The results obtained in Al_2O_3 are reported in Fig. 2. The pump-pulse duration in this case is 70 fs, and the Kerr effect observed at a delay around $t = 0$ gives the pump–probe cross-correlation function. Immediately after this, the phase shift becomes negative and is due to free carriers. The mean lifetime of photoexcited electrons is 100 ps, as measured by the same method [11]. Except for the achieved free carriers density, no noticeable difference can be observed between the data obtained at intensities below and above threshold, indicating that the plasma expansion, or any other ultrafast dramatic modification of the solid, does not perturb our measurements at such a time scale. With the help of (1), we can derive the excitation density corresponding to the observed negative phase shift. If we assume that the density of carriers is homogeneous along the overlapping length (9 μm in this case), we find $8\times10^{19}\,\mathrm{cm}^{-3}$ below and $1.5\times10^{20}\,\mathrm{cm}^{-3}$ above threshold, the intensities are $10^{14}\,\mathrm{W/cm^2}$ and $1.8\times10^{14}\,\mathrm{W/cm^2}$, respectively, whereas the threshold intensity is $1.3\times10^{14}\,\mathrm{W/cm^2}$.

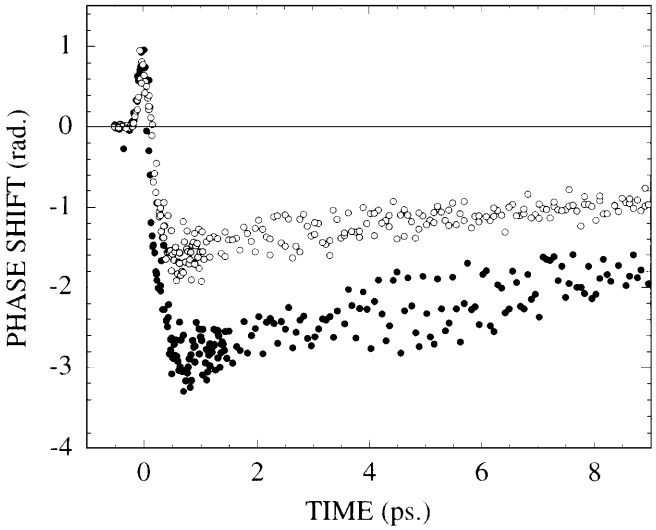

Fig. 2. Phase shift measured in Al_2O_3 as a function of time delay between the pump and the second probe pulses, below ($10^{14}\,\mathrm{W/cm^2}$, *open circles*) and above ($1.8\times10^{14}\,\mathrm{W/cm^2}$, *full circles*) breakdown threshold

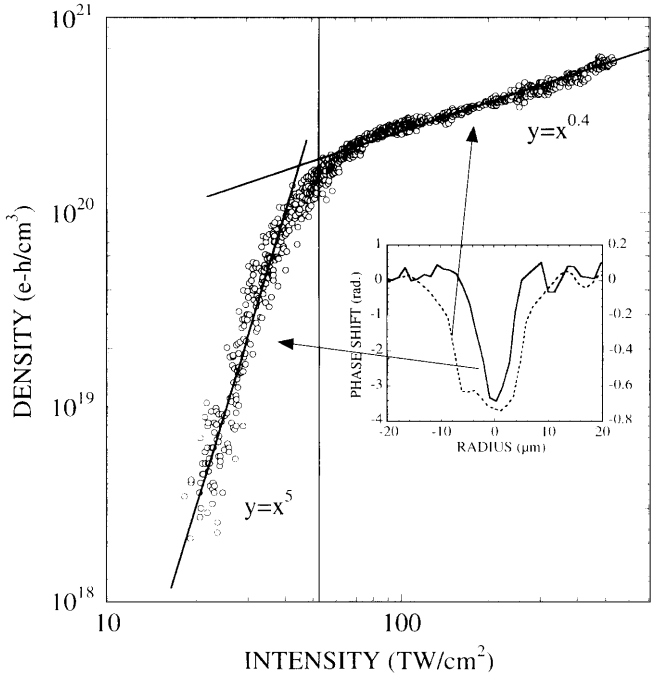

Fig. 3. Excitation density as a function of pump laser intensity in MgO. The *vertical line* indicates the breakdown threshold. The *inset* shows the profile of phase shift for different intensities: note the different scales for the low-intensity *(full line, right scale)* and high-intensity *(dotted line, left scale)* profiles

The next result concerns MgO. Figure 3 is displays the excitation density deduced from the phase shift measurements as a function of intensity, while the absorption is plotted on Fig. 4. The pump pulse duration is 80 fs in this case. At "low" intensity the photogenerated carriers density increases very sharply, and this region can be fitted by a power law I^5. Since the absorption of five pump photons of (1.55 eV) is enough to excite electrons across the 7.5-eV band gap of MgO, this slope of 5 is a strong indication of a multiphoton process of order five. The increase in absorption in the same intensity

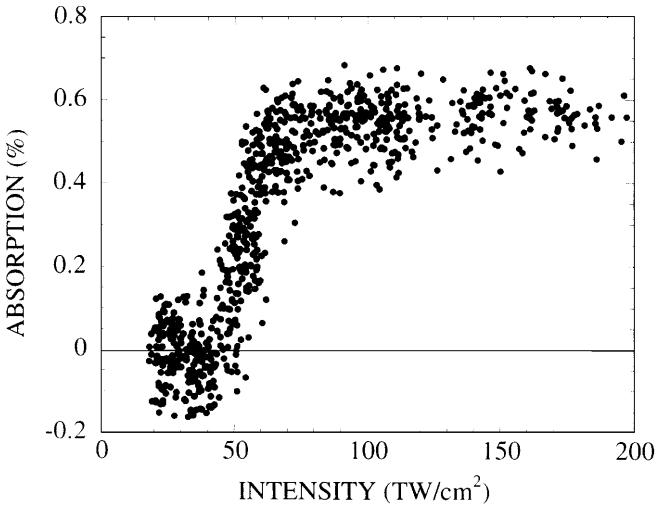

Fig. 4. Absorption as a function of pump laser intensity in MgO

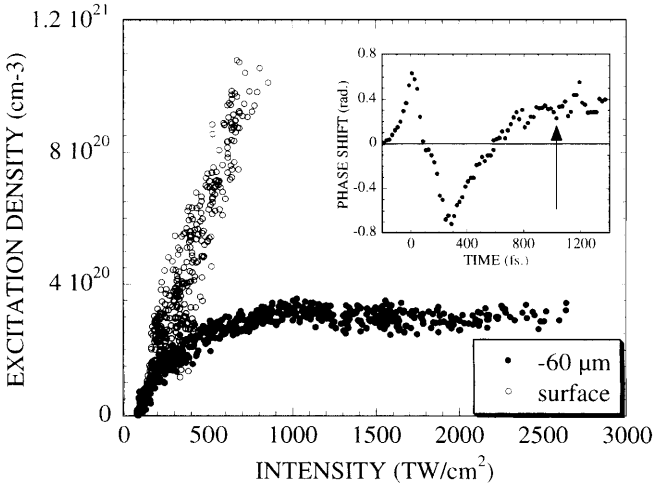

Fig. 5. Excitation density as a function of pump laser intensity in SiO_2, measured at the surface *(open circles)* and 60 μm behind *(full circles)*. The *inset* shows the phase shift as a function of time, and the *arrow* indicates the delay between pump and probe for intensity measurements

range can also be fitted by a fifth-order multiphoton process. Different hypothesis can be put forward to explain the change of slope at higher intensities. It is most probably due to a saturation effect. This can be deduced from the phase-shift profile measured in the two different regimes, displayed in the inset of Fig. 3. The FWHM of the pump beam measured with the Kerr effect, is 8 μm. The profile obtained at low intensity is thinner, because the excitation process is nonlinear. On the contrary the profile at high intensity is broader with a top-hat shape, indicating the saturation effect. Again this saturation may have different origins. It could be a saturation of the ionization process. But in this case we would expect an excitation density in the range of a few times 10^{22} cm^{-3}, contrary to what we observe. The most probable explanation is that a dense plasma is generated in a thin layer inside the solid during the leading edge of the pulse, and that the end of the pulse is reflected by this plasma. Indeed the critical density for the pump wavelength (800 nm) is 2×10^{21} cm^{-3}. The density measured at the change of slope is about ten times weaker. However, this result is an average over the overlap between the pump and probe and over the radius of the pump beam, and it is very probable that this critical density may be reached at the centre of the beam and at the surface of the sample, where the intensity is maximum. Furthermore, this change of slope occurs at the intensity where we noticed the damage threshold. Since our measurement of breakdown indicates a damage of the order of 10% of the size of the pump beam, it is expected that a plasma reaching the critical density is formed at the surface. This criteria was indeed used by Von der Linde and Schüler [9] to define the breakdown threshold for 120 fs pulses.

3 SiO_2

The case of SiO_2 deserves special attention. It has been shown that, as for to alkali halides, electron hole pairs form self-trapped excitons (STE) [12, 13]. This process is very fast and efficient, leading to the trapping of photoexcited carriers in a mean time of 150 fs. This kinetics has been measured both in α-SiO_2 (quartz) and in a-SiO_2 (fused silica) by time-resolved absorption [14] and interferometry [15]. The consequence of this ultrafast trapping is that the phase shift becomes positive in SiO_2 after approximately 500 fs, as shown in the inset of Fig. 5. We show on this figure the excitation density measured 1 ps after the 70 fs pump pulse (as indicated by the arrow in inset) as a function of intensity, at the surface and 60 μm behind. The excitation densities were deduced from the phase shift by using the last term of (1), the parameters for the STE's absorption band being taken from the literature [16, 17]. The measurement at the surface could not be performed at the highest intensities, the probe beam being either completely absorbed or reflected. The intensity of the pump beam itself must be strongly reduced, due to the absorption by STE's or the plasma at the surface, or reflected by this plasma, as we found in MgO. This also explains the saturation observed in the excitation density that could be achieved deeper in the sample. This result clearly demonstrates the advantage of making measurements at a controlled depth. They are, in particular, extremely important for the

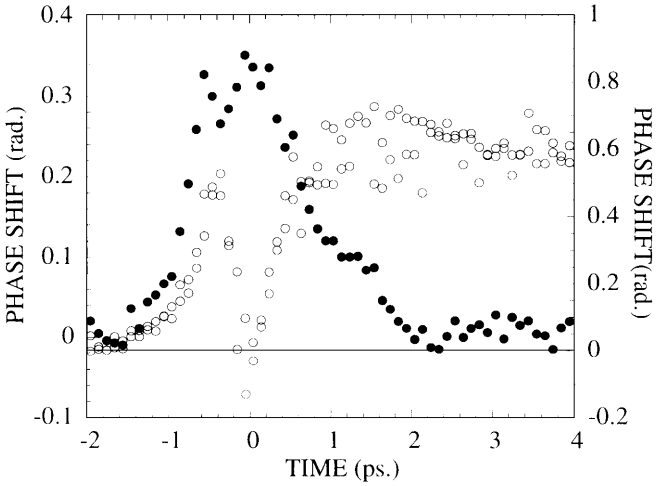

Fig. 6. Phase shift measured in SiO_2 as a function of time delay between the pump and the second probe pulses, at 8×10^{12} W/cm^2 *(full circles, left scale)* and 2.4×10^{13} W/cm^2 *(open circles, right scale)*

understanding and modelling of the propagation of high intensity laser pulses.

Another important effect which may dramatically influence the propagation is illustrated in Fig. 6, where the phase shift is reported as a function of time for two different intensities The full circles were obtained at low intensity (8×10^{12} W/cm^2), where essentially only the Kerr effect is observed. This result gives the temporal profile of the pump pulse (FWHM 1.3 ps). Open circles are measurements at a much higher intensity (2.4×10^{13} W/cm^2). The rise in phase shift is also due to Kerr effect, then the sudden decrease is due to free carriers generated since the beginning of the pump. These carriers are trapped very rapidly to form STEs, leading to the positive phase shift observed well before the end of the pulse.

4 Conclusion

We have reported the first measurements of the excitation density in wide-band-gap insulators during or just after picosecond and subpicosecond laser pulses at intensities below and above breakdown threshold. We believe these new experimental results will be extremely helpful to understanding either the propagation of laser pulses below breakdown threshold or the importance of the fundamental mechanisms involved in the breakdown phenomena. Of course, a full understanding of these experimental data requires some modeling work. However, some general remarks regarding these two aspects can already be formulated.

It is interesting to compare the excitation density measured in the different materials at breakdown threshold intensities. We have reported these values in Fig. 7 for the different pulse durations we used in these experiments. Note that the density of carriers at threshold decreases by one order of magnitude when the pulse duration increases from 70 fs to 1.3 ps.

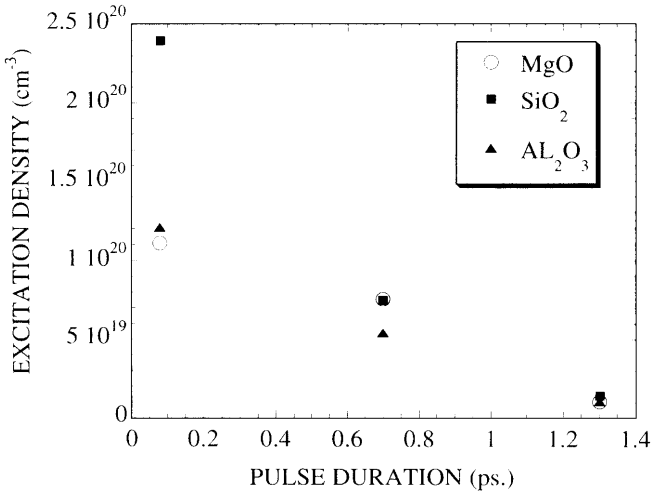

Fig. 7. Excitation density at breakdown threshold for different pulse duration in the three materials

This result suggests that the breakdown threshold should not be defined as the achievement of a critical excitation density. It emphasises the importance of electron heating, as underlined by Jones and co-workers [2]. It would thus be interesting to perform measurements at longer pulse duration, where thermal effects are supposed to play a dominant role.

The strong differences between a material were trapping occurs, SiO_2, and those in which electrons remain in the conduction band during a long time are noteworthy. By comparing Figs. 2 and 6, we see that the change of refractive index is negative in the case of Al_2O_3 and positive in SiO_2. This means that the carriers initially photoexcited will tend to *defocus* the beam in the first case, and to *focus* it in the other case. This aspect will therefore play an extremely important role in the propagation of pulses as soon as their duration exceeds 1 or 2 ps. It has also been shown that a small fraction (about 10^{-4}) of these self-trapped excitons form permanent defects which have a strong absorption at 5.2 eV [14]. It is clear in this context that single- and multiple-shot experiments do not have the same meaning. Indeed when SiO_2 is irradiated at an intensity close to (but below) the threshold, the density of carriers trapped in the band gap will increase continuously, leading to a progressive modification of the optical properties of the solid. Indeed we readily observe in our experiment this coloration of the sample at intensities below breakdown threshold.

Acknowledgements. Richard Deblock and Josselin Philip are gratefully acknowledged for their help in setting up the experiment.

References

1. N. Bloembergen: IEEE J. Quantum Electron. **QE-10**, 375 (1974)
2. S.C. Jones, P. Braunlich, R.T. Casper, X.A. Shen, P. Kelly: Opt. Eng. **28**, 1039 (1989)
3. B.C. Stuart, M.D. Feit, S. Herman, A.M. Rubenchik, B.W. Shore, M.D. Perry: Phys. Rev. B **53**, 1749 (1996)
4. D. Du, X. Liu, G. Korn, J. Squier, G. Mourou: Appl. Phys. Lett. **64**, 3071 (1994)
5. H. Varel, D. Ashkenasi, A. Rosenfeld, R. Herrmann, F. Noack, E.E.B. Campbell: Appl. Phys. A **62**, 293 (1996)
6. M. Lenzner, J. Krüger, S. Sartania, Z. Cheng, Ch. Spielman, G. Mourou, W. Kautek, F. Krausz: Phys. Rev. Lett. **80**, 4076 (1998)
7. X.A. Shen, S.C. Jones, P. Braunlich: Phys. Rev. Lett. **62**, 2711 (1989)
8. Ph. Daguzan, S. Guizard, K. Krastev, P. Martin, G. Petite, A. Dos Santos, A. Antonetti: Phys. Rev. Lett. **73**, 2352 (1994)
9. D. von der Linde, H. Schüler: J. Opt. Soc. Am. B **23**, 216 (1996)
10. P. Martin, S. Guizard, Ph. Daguzan, G. Petite, P. D'Oliveira, P. Meynadier, M. Perdrix: Phys. Rev. B **55**, 5799 (1997)
11. S. Guizard, P. Martin, Ph. Daguzan, G. Petite, P. Audebert, J.P. Geindre, A. Dos Santos, A. Antonetti: Europhys. Lett. **29**, 401 (1995)
12. K. Tanimura, T. Tanaka, N. Itoh: Phys. Rev. Lett. **51**, 423 (1983)
13. W. Hayes, M.J. Kane, O. Salminen, R.L. Wood, S.P. Doherty: J. Phys. C **17**, 2943 (1984)
14. S. Guizard, P. Martin, G. Petite, P. D'Oliveira, P. Meynadier: J. Phys.: Condens. Matter **8**, 1281 (1996)
15. P. Audebert Ph. Daguzan, A. Dos Santos, J.C. Gautier, J.P. Geindre, S. Guizard, G. Hamoniaux, K. Krastev, P. Martin, G. Petite, A. Antonetti: Phys. Rev. Lett. **73**, 1990 (1994)
16. C. Itoh, K. Tanimura, N. Itoh: J. Phys. C **21**, 4693 (1988)
17. T. Tanaka, T. Eshita, K. Tanimura, N. Itoh: Cryst. Latt. Def. Amorph. Mater. **11**, 221 (1985)